2020 IEEE/RSJ International Conference on Intelligent Robots and Systems (IROS)
October 25-29, 2020, Las Vegas, NV, USA (Virtual)

Decentralized Control Schemes for Stable Quadrupedal Locomotion: A Decomposition Approach from Centralized Controllers*

Abhishek Pandala**, Vinay R. Kamidi**, and Kaveh Akbari Hamed

***Abstract*— Although legged robots are becoming more nonlinear with higher degrees of freedom (DOFs), the centralized nonlinear control methods required to achieve stable locomotion cannot scale with the dimensionality of these robots. This paper investigates time-varying decentralized feedback control architectures based on hybrid zero dynamics (HZD) that stabilize dynamic legged locomotion with high degrees of freedom. By conforming to the natural symmetries present in the robot's full-order model, three decentralization schemes are proposed for control synthesis, namely left-right, front-hind and diagonal. Our approach considers the strong nonlinear interactions between the subsystems and relies only on the intrinsic communication of the body's translation and rotational data that is readily available. Further, a quadratic programming (QP) based feedback linearization is employed to compute the control inputs for each subsystem. The effectiveness of the HZD-based decentralization scheme is demonstrated numerically for the stabilization of forward and inplace walking gaits on an 18 DOF robot.**

I. INTRODUCTION

Many centralized and nonlinear control schemes have been developed for stabilizing periodic gaits of legged locomotion. In these approaches, multiple links and joints of the robot communicate their sensor measurements to a central nonlinear controller. This controller interprets the data from all joints and relays decisions back to all actuators. These centralized techniques include the ones based on geometric reduction [1], [2], transverse linearization [3], [4], controlled symmetries [5] and hybrid zero dynamics (HZD) [6]–[12]. Of these, only HZD and transverse linearization can systematically address underactuation, a situation common to dynamic legged locomotion. In fact, a wide class of legged robots have taken advantage of the rigorous controllers synthesized by the HZD for periodic gaits and experimentally demonstrated feasible walking under this framework, e.g., 2D and 3D bipedal robots [7], [13]–[21], 3D powered prosthetic legs [22]–[24], exoskeletons [25], and reduced-order quadrupedal locomotion [26]. These advances render the HZD approach highly attractive and correspondingly persuaded the translation of HZD formulation to full order quadrupedal robots [27], [28].

* The work of A. Pandala and V. R. Kamidi is supported by the NSF under the grant 1854898. The work of K. Akbari Hamed is supported by the National Science Foundation (NSF) under Grant Numbers 1923216 and 1924617. The content is solely the responsibility of the authors and does not necessarily represent the official views of the NSF.

** A. Pandala and V. R. Kamidi contributed equally to this work.

A. Pandala, V. R. Kamidi, and K. Akbari Hamed are with the Department of Mechanical Engineering, Virginia Tech, Blacksburg, VA 24061, USA, {agp19, vinay28, kavehakbarihamed} @vt.edu

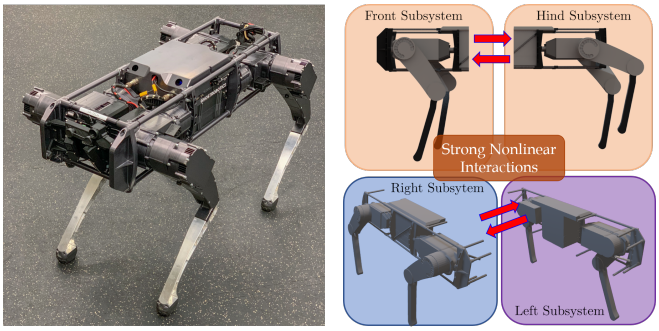

Fig. 1. (Left) Quadrupedal robot, Vision 60, whose full-order and 18-DOF model is considered in this paper for numerical simulations. (Right) Conceptual illustration of the proposed decomposition schemes to synthesize decentralized controllers (Top Right: front-hind decomposition) (Bottom Right: left-right decomposition).

Despite the superior performance of centralized schemes, they exhibit a lack of scalability with the increasing complexity of legged robots. For example, HZD schemes require the inversion of a state-dependent decoupling matrix at every time sample to compute the control inputs. The computational complexity of this operation scales as $O(n^3)$, where n is the number of degrees of freedom (DOFs) [29]. This increasing computational complexity presents one of the key roadblocks to the application of traditional HZD-based centralized controllers to high-DOF systems. Moreover, inverting the decoupling matrix may amplify and distribute local modelling errors across the entire full-order model. In addition to the computational bottlenecks, the system integration required to implement centralized feedback control architectures is also a significant challenge in high-DOF robots. Because a single micro-controller does not have nearly enough I-O channels to integrate all the sensors and actuators of a high-DOF robot, these robots require a sophisticated high-throughput network of computers to achieve centralized computation and control [30].

An alternative school of thought advocates decentralization schemes that preserve rich structural characteristics embedded in higher-order models while simultaneously alleviating the computational burden and minimizing communication between subsystems. A considerable body of research in neurophysiology also indicates the existence of locality in the control architectures of animal locomotion. Specifically, spinal cat experiments have demonstrated that cats are capable of walking with a wide range of gaits on a treadmill after their spinal cord has been severed to isolate the rear legs from the brain and front legs [31]. This motivates the *development and exploitation of decentralization*

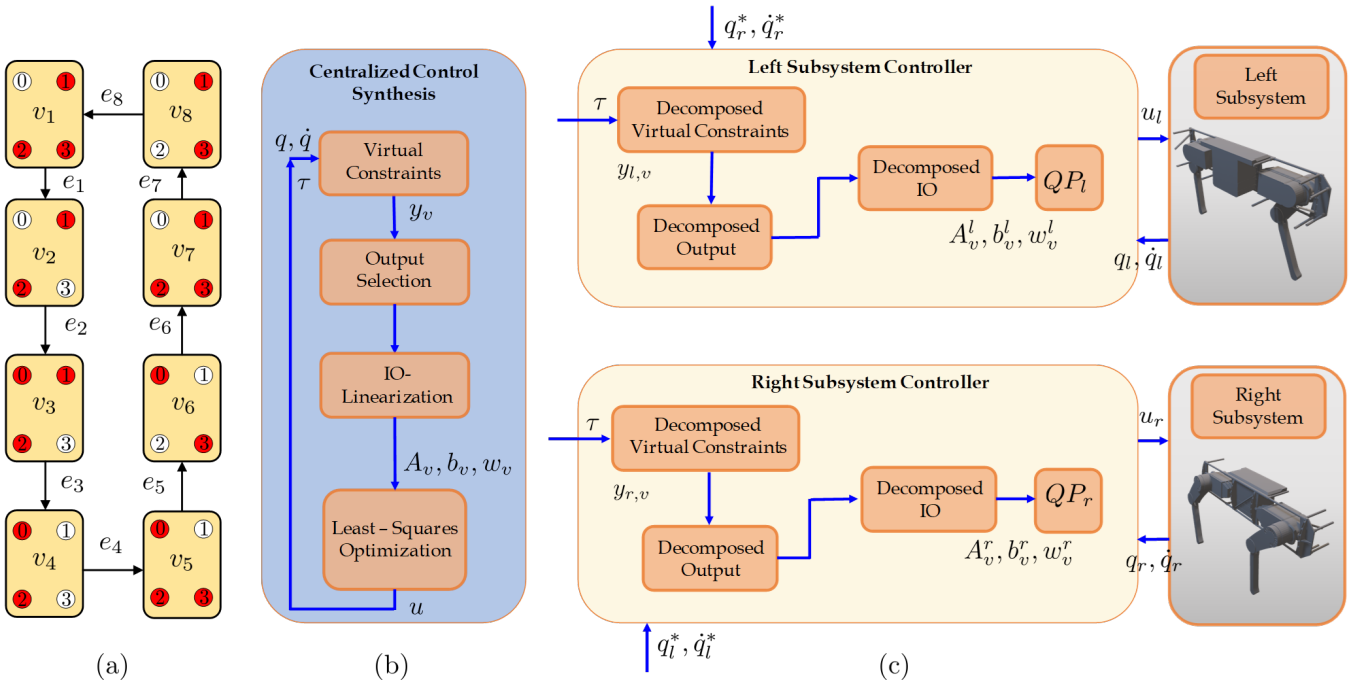

Fig. 2. (a) Illustration of the 8-domain directed graph to describe periodic walking. (b) Schematic representation of the HZD-based centralized control architecture. (c) Illustration of the HZD-based decentralized controllers for 12 DOF, left-right subsystems. A similar schematics can be obtained for both front-hind and diagonal decompositions.

schemes. Design of decentralized controllers presents significant challenges, especially for high-DOF legged robots. Particularly, the existence of strong nonlinear interaction among subsystems, underactuation, and hybrid nature of the dynamical systems exacerbates the task. Furthermore, state-of-the-art decentralized control schemes are tailored to the stabilization of equilibrium points for ordinary differential equations (ODEs) and *not* periodic orbits of hybrid dynamical systems [32].

The objective of this paper is to design time-varying and HZD-based decentralized control schemes that stabilize periodic gaits of quadrupedal locomotion. We present a decomposition approach based on the natural symmetries of the quadrupedal robot, namely left-right symmetry, front-hind symmetry and diagonal symmetry. The dynamics of each subsystem are addressed to set up a feedback linearization based Quadratic Programming (QP) problem that synthesizes local controllers. The proposed approach estimates the nonlinear interactions amongst subsystems by assuming that the other subsystem is on the periodic orbit. This reduces the need for information sharing between subsystems. We validate our HZD-based decentralization control scheme through simulations on forward and inplace walking gaits, using the full-order model of Vision 60, manufactured by GhostRobotics[1] (see Fig. 1). In our previous work [33], [34], we demonstrated the feasibility of time-invariant decentralized algorithms for bipedal locomotion albeit under the assumption that each subsystem has access to position and orientation data from strategically placed additional inertial measurement units (IMUs). The current paper extends the work in [33], [34] to quadrupedal locomotion by 1) proposing decentralized control laws that eliminate the need for communication among subsystems, and 2) extending the decentralized feedback laws to be time-varying. The paper numerically verifies the effectiveness of the proposed approach for synthesizing local HZD controllers for different decentralization schemes. In addition, a robustness analysis is performed to study the resilience of these schemes against external disturbances.

[1] https://www.ghostrobotics.io/

II. PRELIMINARIES

A. System Description and Robot Model

Vision 60 is an $n = 18$-DOF quadrupedal robot with $m = 12$ actuators. To provide a complete mechanical description of the robot, we consider the inertial world frame $\{O\}$ and a base frame $\{B\}$ that is rigidly attached to the geometric centre of the robot. The Cartesian position associated with the three translational DOFs of the robot is represented by $p_b \in \mathbb{R}^3$. Correspondingly the three rotational DOFs with respect to $\{O\}$ are encoded in $\phi_b \in \mathrm{SO}(3)$ and are cumulatively parameterized by $\vartheta := \mathrm{col}(p_b, \phi_b)$. The remaining 12-DOFs are the actuated joints that define the robot's shape variables and are denoted by $q_{act} \in \mathbb{R}^m$. In particular, each leg of the robot has 3-DOFs: 2-DOFs at the hip for the roll and pitch motion together with a 1-DOF knee. The generalized coordinates are then defined by $q := \mathrm{col}(\vartheta, q_{act}) \in \mathcal{Q}$, where $\mathcal{Q}$ represents the configuration space. Subsequently, the state vector is taken as $x := \mathrm{col}(q, \dot{q}) \in \mathcal{X} := \mathrm{T}\mathcal{Q}$, where $\mathcal{X}$ is the state manifold and $\mathrm{T}\mathcal{Q}$ denotes the tangent bundle of $\mathcal{Q}$.

B. Hybrid Dynamic Framework for Legged Locomotion

Throughout this work, we will refer to the hybrid model of the quadrupedal locomotion by the following tuple

$$\Sigma := (\mathcal{G}, \mathcal{D}, \mathcal{S}, \Delta, \mathcal{FG}), \tag{1}$$

where $\mathcal{G} = (\mathcal{V}, \mathcal{E})$ is the directed cycle with the vertex set $\mathcal{V} := \{v_1, ..., v_k\}$ and edge set $\mathcal{E} := \{e_1, ..., e_k\}$ (see Fig. 2(a)). In our formulation, $\mathcal{D}$ is the set of admissible domains on which the unilateral constraints are met and ground reaction forces are feasible, $\mathcal{S} := \{\mathcal{S}_e\}_{e\in\mathcal{E}}$ is the set of switching surfaces, referred to as the guards of the hybrid system, and $\Delta := \{\Delta_e\}_{e\in\mathcal{E}}$ is the set of reset laws that describe discrete-time transitions triggered on $\mathcal{S}_e$. Finally, $\mathcal{FG} := \{(f_v, g_v)\}_{v\in\mathcal{V}}$ represents the set of control systems on $\mathcal{D}$, defined by the affine control system $\dot{x} = f_v(x) + g_v(x)\,u$, for all $(x, u) \in \mathcal{D}$. The notion of hybrid dynamics is further detailed in [27], [35].

C. Continuous-Time Dynamics

The evolution of the robot in each domain $v \in \mathcal{V}$ can be described by Euler-Lagrange equations and the principle of virtual work as follows:

$$D(q)\,\ddot{q} + H(q,\dot{q}) \quad = B\,u + J_v^\top(q)\,\lambda \tag{2}$$

$$J_v(q)\,\ddot{q} + \dot{J}_v(q,\dot{q})\,\dot{q} = 0, \tag{3}$$

where $D(q) \in \mathbb{R}^{n\times n}$ is the positive definite mass-inertia matrix, $H(q,\dot{q}) := C(q,\dot{q})\,\dot{q} + G(q) \in \mathbb{R}^n$ represents the coriolis and gravitational terms, $B \in \mathbb{R}^{n\times m}$ is the input distribution matrix, λ represents the ground reaction forces, and J_v is the contact Jacobian matrix.

D. Discrete-Time Dynamics

Every time the robot makes or breaks contact with the environment, a discrete-time transition occurs. Whenever the robot breaks a contact, the discrete-time transition is simply taken as the identity map, i.e., $x^+ = \Delta_e(x^-) = x^-$. During contact initiation, the state of the robot, specifically the velocities undergo an abrupt change according to the instantaneous impact model between two rigid bodies [36]. The evolution of the system during the infinitesimal contact initiation can be given by

$$D(q)\,\dot{q}^+ - D(q)\,\dot{q}^- = J_{v+1}^\top(q)\,\delta\lambda, \quad J_{v+1}(q)\,\dot{q}^+ = 0. \tag{4}$$

Here, $\dot{q}^+, \dot{q}^-$ are the generalized velocities right after and before impact, $\delta\lambda$ represents the intensity of the impulsive ground reaction forces during the impact, and the contact Jacobian matrix J_{v+1} corresponds to the domain right after impact. Assuming the continuity of position ($q^+ = q^-$), the state of the robot after the impact can be computed from (4) as a discrete-time map by $x^+ = \Delta_e(x^-)$.

III. HZD-BASED CENTRALIZED CONTROL

The proposed decentralization structure depends on the decomposition of stabilizing centralized controllers. The objective of this section is to develop time-varying and centralized virtual constraint controllers that stabilize dynamic gaits for the hybrid model of locomotion. The decentralized versions of these controllers will be addressed in Section IV.

Virtual constraints [6], [8] are a set of kinematic constraints that can be imposed by the action of feedback control laws to coordinate the motion of links during locomotion. In this work, we consider the following time-varying virtual constraints for the domain $v \in \mathcal{V}$

$$y_v(\tau, x) := h_v^0(q) - h_v^d(\tau). \tag{5}$$

Here, $h_v^0(q)$ and $h_v^d(\tau)$ represent the set of holonomic functions to be controlled and their corresponding desired evolution on the gait, respectively. Furthermore, τ denotes the gait timing (i.e., phasing) variable which represents the progress of the robot on the gait. In particular, it is taken as zero at the beginning of each domain (i.e., $\tau^+ = 0$) and then evolves according to

$$\dot{\tau} = \frac{1}{t_v^d} \tag{6}$$

where t_v^d is the desired elapsed time for the domain v. We would like the controller to be able to track the absolute position and orientation of the robot's base together with pre-planned foot trajectories. In order to achieve this, the first six holonomic functions are chosen as the COM position and absolute orientation. The rest of the holomonic outputs are chosen to regulate the Cartesian coordinates of the swing leg end-effectors.

Complying with the standard I-O linerization [37], the output dynamics become

$$\ddot{y}_v := L_{g_v} L_{f_v} y_v(\tau, x)\,u + L_{f_v}^2 y_v(\tau, x), \tag{7}$$

where the right-hand side of equation (7) can be written as $A_v(t,x)\,u + b_v(t,x)$ with $A_v := L_{g_v} L_{f_v} y_v$ and $b_v := L_{f_v}^2 y_v$. We are now interested in having the following desired output dynamics

$$\ddot{y}_v = -k_p y_v - k_d \dot{y}_v =: w_v(\tau, x), \tag{8}$$

where k_p and k_d are positive gains. From (8), the minimum-power (i.e., least-square) state feedback law that results in the asymptotic output tracking can be obtained as follows:

$$u = \Gamma_v(\tau, x) := -A_v^\top (A_v A_v^\top)^{-1}(b_v - w_v). \tag{9}$$

The feasibility of torques u cannot be guaranteed by the minimum-power control law in (9). To this end, one can alternatively formulate the centralized control synthesis problem as the following QP:

$$\begin{aligned} \underset{(u,\delta)}{\arg\min} \quad & \frac{1}{2}||u||_2^2 + \frac{\varpi}{2}||\delta||_2^2 \\ s.t. \quad & A_v u + \delta = w_v - b_v \\ & u_{\min} \le u \le u_{\max} \\ & \delta_{\min} \le \delta \le \delta_{\max}. \end{aligned} \tag{10}$$

Here, a slack variable δ is introduced to ensure feasibility of the QP, whenever A_v is not full rank. To minimize the effect of the slack variable δ, a high gain ϖ is chosen accordingly. Further, upper $(u_{\max}, \delta_{\max})$ and lower $(u_{\min}, \delta_{\min})$ bounds on the control input and slack variable are added to ensure feasibility.

IV. HZD-BASED DECENTRALIZED CONTROL

The objective of this section is to present the HZD-based decentralized controllers to asymptotically stabilize dynamic quadrupedal locomotion. In particular, we exploit the natural symmetry present in the robot's full-order model and partition it into three decompositions, **left-right**, **front-hind** and **diagonal**. We remark that all local subsystems in the aforementioned decomposition schemes include two legs of the robot and we will design local controllers for all individual subsystems. Here, we present the control synthesis for the left-right decentralization scheme. The decentralized controllers for the other decompositions can be obtained similarly and will be discussed in Section V.

A. Left-Right Decomposition

This section eliminates the need for full-order model knowledge for the purposes of control synthesis by the construction of two subsystems under the *left-right decomposition* scheme (see Fig. 1). We assume that both subsystems have access to the absolute positions and orientations of the body frame B that are encoded in vectors ϑ and $\dot{\vartheta}$. This ensures each subsystem is aware of its own contribution to the cumulative goal of locomotion. However, there is no other variable sharing/communication between the local controllers. Consequently, the configuration variables for the left subsystem can be represented by $q_l := \text{col}(\vartheta, q_1, q_2, q_3, q_4, q_5, q_6)$, where, $(q_1, ..., q_6)$ are the six actuated DOFs that parameterize the two legs on the left half of the robot. Similarly, $q_r := \text{col}(\vartheta, q_7, q_8, q_9, q_{10}, q_{11}, q_{12})$ and likewise, $(q_7, ..., q_{12})$ denote the six actuated DOFs of the two legs on the right half of the robot.

Note that each individual subsystem has 12-dimensional generalized coordinates, i.e., $q_l \in \mathbb{R}^{12}$ and $q_r \in \mathbb{R}^{12}$ as they both share the 6-dimensional ϑ vector for the global coordinates of the body. Furthermore, the corresponding state variables are taken as $x_l := \text{col}(q_l, \dot{q}_l) \in \mathbb{R}^{24}$ and $x_r := \text{col}(q_r, \dot{q}_r) \in \mathbb{R}^{24}$. The decomposition of the control vector is straight forward and follows the same convention. This will result in $u_l \in \mathbb{R}^6$ and $u_r \in \mathbb{R}^6$ that correspond to the actuated joints in the respective subsystems (see Fig. 2(b)).

B. Continuous-Time Subsystem Dynamics

We can now proceed to separate the individual subsystem's continuous-time dynamics and capture its evolution during domain $v \in \mathcal{V}$. We rewrite (2) and (3) as

$$D(q)\,\ddot{q} + F^v(q, \dot{q}) = T^v(q)\,u, \tag{11}$$

where the definitions of F^v and T^v are readily available in [27]. For the left subsystem, the dynamics of the entire robot are computed using (11) with the estimated configuration vector $\hat{q} := \text{col}(q_l, q_r^*) \in \mathbb{R}^{18}$, where $q_r^* := \text{col}(q_7^*, q_8^*, q_9^*, q_{10}^*, q_{11}^*, q_{12}^*) \in \mathbb{R}^6$ represents the desired evolution of the six actuated DOFs of the right subsystem. In particular, the left subsystem assumes that the right subsystem is on the desired periodic orbit. This assumption lets us estimate the strong nonlinear interactions between the subsystems. We observe in simulations that failure to account for these interactions in the decentralized control synthesis leads to instability. Now, the entire dynamics of the robot can be estimated as

$$\begin{bmatrix} D_{ll} & D_{lr} \\ D_{rl} & D_{rr} \end{bmatrix} \begin{bmatrix} \ddot{q}_l \\ \ddot{q}_r^* \end{bmatrix} + \begin{bmatrix} F_l^v \\ F_r^v \end{bmatrix} = \begin{bmatrix} T_{ll}^v & T_{lr}^v \\ T_{rl}^v & T_{rr}^v \end{bmatrix} \begin{bmatrix} u_l \\ u_r^* \end{bmatrix}, \tag{12}$$

where the dynamic terms D, F^v and T^v are evaluated at $(\hat{q}, \hat{\dot{q}})$. Eliminating $\ddot{q}_r^*$ from the above equations, we get the dynamics of the left subsystem as follows:

$$\hat{D}_{ll}\,\ddot{q}_l + \hat{F}_l^v = \hat{T}_{ll}^v\,u_l, \tag{13}$$

in which $\hat{D}_{ll} := D_{ll} - D_{lr}D_{rr}^{-1}D_{rl}$, $\hat{F}_l^v := F_l^v - D_{lr}D_{rr}^{-1}F_r^v - (T_{lr}^v - D_{lr}D_{rr}^{-1}T_{rr}^v)\,u_r^*$, $\hat{T}_{ll}^v := T_{ll}^v - D_{lr}D_{rr}^{-1}T_{rl}^v$, and u_r^* are the desired control inputs (i.e., feedforward) for the right subsystem. Similar dynamics can be obtained for the right subsystem as well.

C. HZD-Based Decomposition for Local Control

This section describes decentralized controllers that individually work towards the stabilization of dynamic gaits.

Local Outputs Selection: Similar to the holonomic outputs of the centralized controller, we choose to regulate the absolute position and orientation of the robot's base together with the end-effector of the individual subsystem's swing legs. In particular, when both the legs of an individual subsystem are in stance phase, the COM position and the absolute orientation of the robot's base are chosen as holonomic outputs. These holonomic outputs are further augmented with the Cartesian coordinates of the swing foot when the subsystem is in single-contact domain. When both the legs of the subsystem are in swing phase (i.e., flight phase), only the Cartesian coordinates of the swing foot end-effectors are chosen as holonomic outputs. The idea is to regulate the robot's position and orientation only when there is at least one stance leg. With this choice, the local output functions for the left subsystem can be written as follows:

$$y_{lv}(\tau) := h_{lv}^0(q_l) - h_{lv}^d(\tau), \tag{14}$$

where $h_{lv}^0(q_l)$ and $h_{lv}^d(\tau)$ denote the local controlled variables and their desired evolutions on the gait, respectively.

Local QPs and HZD Controllers: Following the same procedure as in section III and rearranging (7) and (8), the local outputs (14) can be linearized along the local dynamics (13) as follows:

$$\underbrace{L_{\hat{g}_v} L_{\hat{f}_v}\, y_{lv}}_{A_v^l(t,x_l)}\, u_l = \underbrace{-k_p\, y_{lv} - k_d\, \dot{y}_{lv}}_{w_v^l(t,x_l)} - \underbrace{L_{\hat{f}_v}^2\, y_{lv}}_{b_v^l(t,x_l)}, \tag{15}$$

where $\dot{x}_l = \hat{f}_v(x_l) + \hat{g}_v(x_l)\,u_l$ represents the state space form of (13). Similar equations can be obtained for the right subsystem. Now, we are in a position to to set up the decentralized QPs that generate local control inputs for each

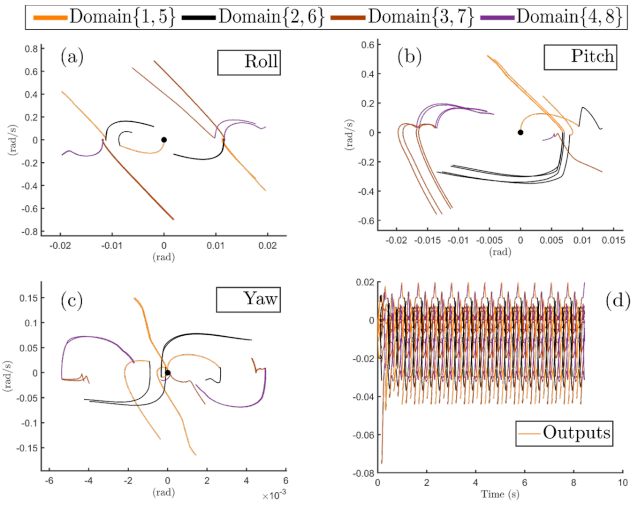

Fig. 3. Illustration of the centralized controller's performance over 35 cycles: (a) Limit cycle convergence of the body roll (b) Limit cycle convergence of the body pitch (c) Limit cycle convergence of the body yaw (d) Time profile of virtual constraints over 15 cycles.

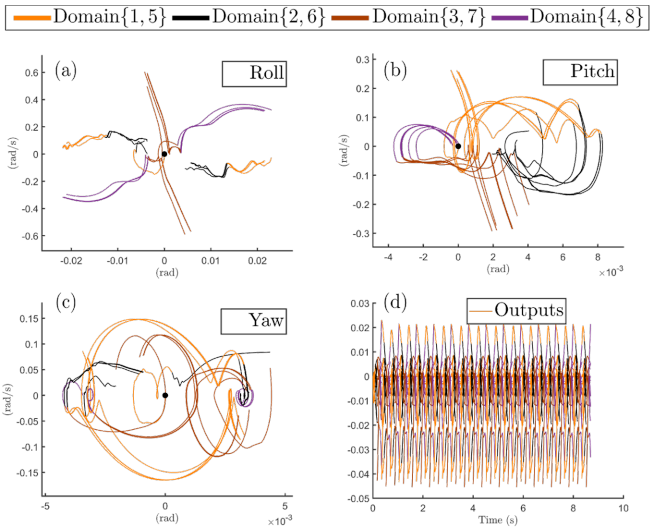

Fig. 4. Left-Right decentralized control scheme performance over 35 cycles on forward walking gait: (a) limit cycle convergence of body roll (b) Body pitch phase portrait (c) Yaw phase portrait (d) Time profile of local virtual constraints over 15 cycles.

subsystem by imposing local virtual constraints as:

$$\begin{aligned} \underset{(u_l,\delta_l)}{\arg\min} \quad & \frac{1}{2} \parallel u_l \parallel_2^2 + \frac{\varpi_l}{2} \parallel \delta_l \parallel_2^2 \\ s.t. \quad & A_v^l u + \delta = w_v^l - b_v^l \\ & u_{l,\min} \leq u_l \leq u_{l,\max} \\ & \delta_{l,\min} \leq \delta_l \leq \delta_{l,\max}. \end{aligned} \tag{16}$$

The definitions of A_v^l, b_v^l, and w_v^l are taken from (15) and are analogous to (10). In addition, ϖ_l is introduced to minimize the effect of the slack variable δ_l. Similarly, one may reformulate (16) for the right subsystem to compute the corresponding local control.

V. NUMERICAL SIMULATIONS

The objective of this section is to demonstrate the effectiveness of the proposed methodology through extensive numerical simulations.

A. Gait Planning

This paper studies inplace and forward walking gaits in quadrupedal locomotion that consists of 8 continuous time domains (see Fig. 2(a)). A 0.15 (m/s) gait is designed utilizing the Hermite-Simpson based direct collocation approach exploited in the FROST (Fast Robot Optimization and Simulation Toolkit) framework [38]. We utilize the resultant gait as a reference trajectory to evaluate all the proposed decentralized controllers. The gait planning in FROST is transcribed into a nonlinear programming (NLP) problem which is readily addressable by the IPOPT solver [39]. The centralized HZD controller synthesized in section III with the optimized output matrices results in asymptotic stability of the gait as shown in Fig. 3. The convergence of limit cycles is clearly illustrated in Fig.3 (a-c).

B. QP based Decentralized Controller

We next implement the proposed decentralized controllers on different decomposition schemes at a control frequency of 1kHz, utilizing qpSWIFT [40]. In what follows, we provide the results for the aforementioned decentralized schemes.

Figure 4 (a-c) shows the body roll, pitch and yaw phase portraits for the Left-Right decentralization scheme in forward walking gait. Figure 4 (d) depicts the time profile of combined outputs for both subsystems. Figures 5 and 6 represent the same plots for front-hind and diagonal decentralization schemes respectively. A clear convergence to a limit cycle in all of the decentralization schemes can be observed. In the interest of space, graphical results for inplace walking gait are not presented here, but can be readily found in the accompanying video.

C. Robustness of Decentralization Schemes

The objective of this section is to evaluate the proposed decentralization schemes in the presence of external disturbances. For this purpose, each of the three decentralized controllers along with the centralized controller are evaluated by perturbing the dynamical system with a constant external force of $250N$ in the y-direction at the geometric center of the robot. Figure 7 shows the phase portraits of the pitch angle of the robot's base for a forward walking gait. It can be observed from Fig. 7 (a) and (d) that the phase portraits of front-hind decentralization scheme and the centralized controller are in the same range, indicating similar performance for both controllers. This can be attributed to the presence of at-least one stance leg for both the subsystems across all the domains of the walking gait in the front-hind decentralization scheme. However, this is not the case for left-right and diagonal decentralization schemes. The presence of stance legs in all domains enabled the front-hind decentralization

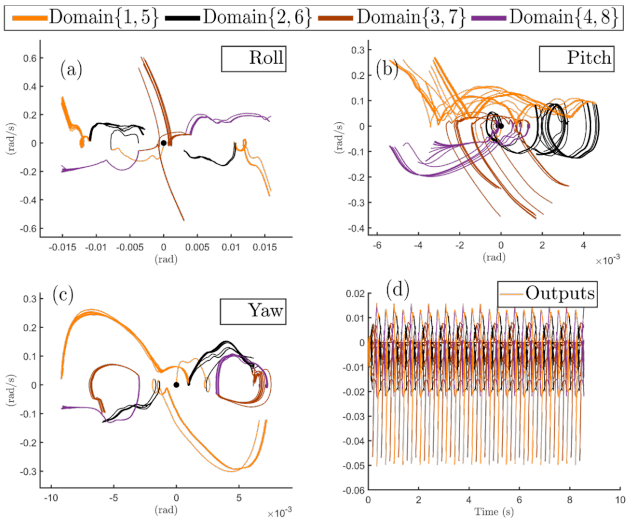

Fig. 5. Front-Hind decentralized control scheme performance over 35 cycles on forward walking gait: (a) limit cycle convergence of the body roll (b) Body pitch phase portrait (c) Yaw phase portrait (d) Time profile of local virtual constraints over 15 cycles.

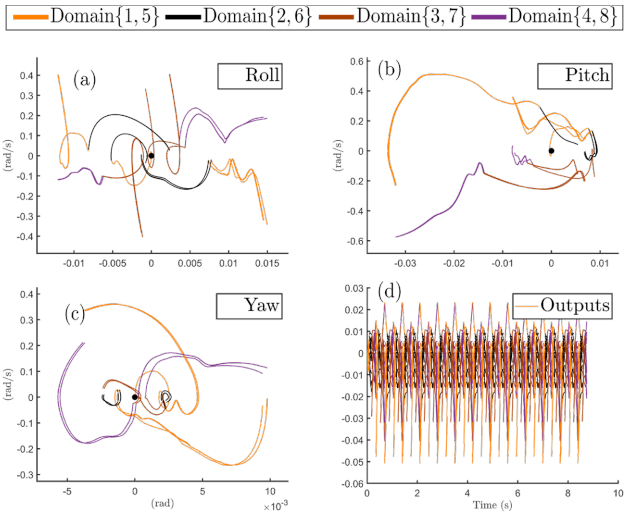

Fig. 6. Diagonal decentralized control scheme performance over 35 cycles on forward walking gait: (a) limit cycle convergence of the body roll (b) Body pitch phase portrait (c) Yaw phase portrait (d) Time profile of local virtual constraints over 15 cycles.

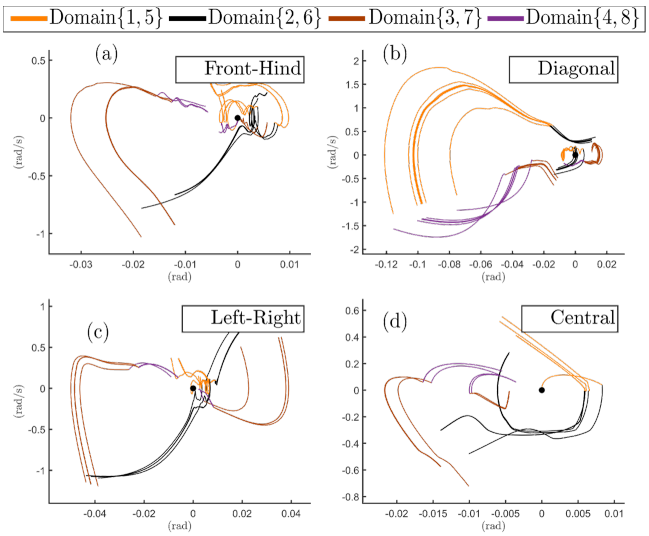

Fig. 7. Pitch phase portrait of various control schemes with external disturbances on forward walking gait: (a) Front-hind decentralization scheme (b) Diagonal decentralization scheme (c) Left-right decentralization scheme (d) Centralized control scheme.

strategy to better regulate the body orientation in comparison to other decentralization strategies.

VI. CONCLUSIONS

This paper introduced a decomposition approach for synthesizing HZD-based decentralized controllers that stabilize periodic orbits for quadrupedal locomotion. In contrast to the existing approaches, the proposed methods *are not constrained on the availability of any additional information* (e.g., the orientation of each subsystem from external IMUs). We avail the fact that the already existing IMU is common to both the subsystems and the exploitation of this property leads to the notion of *no information sharing*. Further, by conforming to the natural symmetries of the robot's dynamic model, the original 36-dimensional full-order model is decomposed into two 24-dimensional subsystems. Similar decomposition structure was then imparted on the dynamics as a precursor for developing individual subsystem controllers. Finally, a layer of safety for each subsystem, in the form of QP was imposed to account for the strong interactions that arise due to decentralization. The potential of the decentralization scheme was then illustrated by demonstrating asymptotically stable periodic forward and inplace walking gaits. The paper numerically demonstrated that the proposed controller synthesis approach can systematically stabilize locomotion patterns for three different decentralization schemes: left-right, front-hind, and diagonal decompositions.

We have also observed that with the existing walking gaits and the choice of output functions, the front-hind decentralization scheme shows better performance in comparison to other decentralization schemes. Future work will investigate alternative decomposition schemes, one example of which is considering each leg as a separate subsystem. Additionally, we wish to rigorously study and address the ramifications of decentralization on different quadrupedal gaits such as ambling, trotting, and bounding. From an experimental standpoint, we will evaluate the performance of the proposed decentralized controllers on a quadrupedal robot.

REFERENCES

[1] A. D. Ames, R. D. Gregg, E. D. B. Wendel, and S. Sastry, "On the geometric reduction of controlled three-dimensional bipedal robotic walkers," in *3rd Workshop on Lagrangian and Hamiltonian Methods for Nonlinear Control*, 2006.

[2] R. D. Gregg and M. W. Spong, "Reduction-based control of three-dimensional bipedal walking robots," *The International Journal of Robotics Research*, vol. 29, no. 6, pp. 680–702, May 2010.

[3] A. Shiriaev, L. Freidovich, and S. Gusev, "Transverse linearization for controlled mechanical systems with several passive degrees of freedom," *Automatic Control, IEEE Transactions on*, vol. 55, no. 4, pp. 893–906, April 2010.

[4] I. R. Manchester, U. Mettin, F. Iida, and R. Tedrake, "Stable dynamic walking over uneven terrain," *The International Journal of Robotics Research*, vol. 30, no. 3, pp. 265–279, 2011.

[5] M. Spong and F. Bullo, "Controlled symmetries and passive walking," *Automatic Control, IEEE Transactions on*, vol. 50, no. 7, pp. 1025–1031, July 2005.

[6] E. Westervelt, J. Grizzle, C. Chevallereau, J. Choi, and B. Morris, *Feedback Control of Dynamic Bipedal Robot Locomotion*. Taylor & Francis/CRC, 2007.

[7] E. Westervelt, J. Grizzle, and D. Koditschek, "Hybrid zero dynamics of planar biped walkers," *Automatic Control, IEEE Transactions on*, vol. 48, no. 1, pp. 42–56, Jan 2003.

[8] J. Grizzle, G. Abba, and F. Plestan, "Asymptotically stable walking for biped robots: Analysis via systems with impulse effects," *Automatic Control, IEEE Transactions on*, vol. 46, no. 1, pp. 51–64, Jan 2001.

[9] B. Morris and J. Grizzle, "Hybrid invariant manifolds in systems with impulse effects with application to periodic locomotion in bipedal robots," *Automatic Control, IEEE Transactions on*, vol. 54, no. 8, pp. 1751–1764, Aug 2009.

[10] A. Ames, K. Galloway, K. Sreenath, and J. Grizzle, "Rapidly exponentially stabilizing control Lyapunov functions and hybrid zero dynamics," *Automatic Control, IEEE Transactions on*, vol. 59, no. 4, pp. 876–891, April 2014.

[11] A. D. Ames, P. Tabuada, A. Jones, W.-L. Ma, M. Rungger, B. Schürmann, S. Kolathaya, and J. W. Grizzle, "First steps toward formal controller synthesis for bipedal robots with experimental implementation," *Nonlinear Analysis: Hybrid Systems*, vol. 25, pp. 155–173, 2017.

[12] K. Akbari Hamed and A. D. Ames, "Nonholonomic hybrid zero dynamics for the stabilization of periodic orbits: Application to underactuated robotic walking," *IEEE Transactions on Control Systems Technology*, 2019.

[13] C. Chevallereau, G. Abba, Y. Aoustin, F. Plestan, E. Westervelt, C. Canudas-de Wit, and J. Grizzle, "RABBIT: A testbed for advanced control theory," *Control Systems Magazine, IEEE*, vol. 23, no. 5, pp. 57–79, Oct 2003.

[14] C. O. Saglam and K. Byl, "Meshing hybrid zero dynamics for rough terrain walking," in *2015 IEEE International Conference on Robotics and Automation (ICRA)*, May 2015, pp. 5718–5725.

[15] A. E. Martin, D. C. Post, and J. P. Schmiedeler, "The effects of foot geometric properties on the gait of planar bipeds walking under HZD-based control," *The International Journal of Robotics Research*, vol. 33, no. 12, pp. 1530–1543, 2014.

[16] K. Sreenath, H.-W. Park, I. Poulakakis, and J. W. Grizzle, "Compliant hybrid zero dynamics controller for achieving stable, efficient and fast bipedal walking on MABEL," *The International Journal of Robotics Research*, vol. 30, no. 9, pp. 1170–1193, Aug. 2011.

[17] K. Sreenath, H.-W. Park, I. Poulakakis, and J. Grizzle, "Embedding active force control within the compliant hybrid zero dynamics to achieve stable, fast running on MABEL," *The International Journal of Robotics Research*, vol. 32, no. 3, pp. 324–345, 2013.

[18] A. Hereid, C. M. Hubicki, E. A. Cousineau, and A. D. Ames, "Dynamic humanoid locomotion: A scalable formulation for HZD gait optimization," *IEEE Transactions on Robotics*, pp. 1–18, 2018.

[19] B. Buss, K. Akbari Hamed, B. A. Griffin, and J. W. Grizzle, "Experimental results for 3D bipedal robot walking based on systematic optimization of virtual constraints," in *2016 American Control Conference (ACC)*, July 2016, pp. 4785–4792.

[20] A. Ramezani, J. Hurst, K. Akbai Hamed, and J. Grizzle, "Performance analysis and feedback control of ATRIAS, a three-dimensional bipedal robot," *Journal of Dynamic Systems, Measurement, and Control December, ASME*, vol. 136, no. 2, December 2013.

[21] S. Veer, M. S. Motahar, and I. Poulakakis, "On the adaptation of dynamic walking to persistent external forcing using hybrid zero dynamics control," in *2015 IEEE/RSJ International Conference on Intelligent Robots and Systems (IROS)*. IEEE, 2015, pp. 997–1003.

[22] H. Zhao, J. Horn, J. Reher, V. Paredes, and A. D. Ames, "First steps toward translating robotic walking to prostheses: a nonlinear optimization based control approach," *Autonomous Robots*, vol. 41, no. 3, pp. 725–742, Mar 2017.

[23] R. Gregg and J. Sensinger, "Towards biomimetic virtual constraint control of a powered prosthetic leg," *Control Systems Technology, IEEE Transactions on*, vol. 22, no. 1, pp. 246–254, Jan 2014.

[24] A. E. Martin and R. D. Gregg, "Stable, robust hybrid zero dynamics control of powered lower-limb prostheses," *IEEE Transactions on Automatic Control*, vol. 62, no. 8, pp. 3930–3942, 2017.

[25] A. Agrawal, O. Harib, A. Hereid, S. Finet, M. Masselin, L. Praly, A. D. Ames, K. Sreenath, and J. W. Grizzle, "First steps towards translating hzd control of bipedal robots to decentralized control of exoskeletons," *IEEE Access*, vol. 5, pp. 9919–9934, 2017.

[26] Q. Cao and I. Poulakakis, "Quadrupedal running with a flexible torso: control and speed transitions with sums-of-squares verification," *Artificial Life and Robotics*, vol. 21, no. 4, pp. 384–392, Dec 2016.

[27] K. Akbari Hamed, W. Ma, and A. D. Ames, "Dynamically stable 3D quadrupedal walking with multi-domain hybrid system models and virtual constraint controllers," in *2019 American Control Conference (ACC)*, July 2019, pp. 4588–4595.

[28] K. Akbari Hamed, J. Kim, and A. Pandala, "Quadrupedal locomotion via event-based predictive control and QP-based virtual constraints," *IEEE Robotics and Automation Letters*, vol. 5, no. 3, pp. 4463–4470, July 2020.

[29] G. W. Stewart, *Matrix Algorithms: Volume 1: Basic Decompositions*. Siam, 1998, vol. 1.

[30] N. Radford et al., "Valkyrie: NASA's first bipedal humanoid robot," *Journal of Field Robotics*, vol. 32, no. 3, pp. 397–419, 2015.

[31] M. Donner, *Real-Time Control of Walking*. Birkhäuser Boston, 1987.

[32] D. Siljak, *Decentralized Control of Complex Systems*. Dover Publications, December 2011.

[33] K. Akbari Hamed and R. D. Gregg, "Decentralized event-based controllers for robust stabilization of hybrid periodic orbits: Application to underactuated 3-d bipedal walking," *IEEE Transactions on Automatic Control*, vol. 64, no. 6, pp. 2266–2281, June 2019.

[34] K. Akbari Hamed and R. D. Gregg, "Decentralized feedback controllers for robust stabilization of periodic orbits of hybrid systems: Application to bipedal walking," *Control Systems Technology, IEEE Transactions on*, vol. 25, no. 4, pp. 1153–1167, July 2017.

[35] A. Ames, "Human-inspired control of bipedal walking robots," *Automatic Control, IEEE Transactions on*, vol. 59, no. 5, pp. 1115–1130, May 2014.

[36] Y. Hurmuzlu and D. B. Marghitu, "Rigid body collisions of planar kinematic chains with multiple contact points," *The International Journal of Robotics Research*, vol. 13, no. 1, pp. 82–92, 1994.

[37] A. Isidori, *Nonlinear Control Systems*. Springer; 3rd edition, 1995.

[38] A. Hereid and A. D. Ames, "Frost: Fast robot optimization and simulation toolkit," in *IEEE/RSJ International Conference on Intelligent Robots and Systems (IROS)*. Vancouver, BC, Canada: IEEE/RSJ, Sep. 2017.

[39] A. Wächter and L. T. Biegler, "On the implementation of an interior-point filter line-search algorithm for large-scale nonlinear programming," *Mathematical programming*, vol. 106, no. 1, pp. 25–57, 2006.

[40] A. G. Pandala, Y. Ding, and H. Park, "qpSWIFT: A real-time sparse quadratic program solver for robotic applications," *IEEE Robotics and Automation Letters*, vol. 4, no. 4, pp. 3355–3362, Oct 2019.